

Scienxt Journal of Mechanical Engineering & Technology
Volume-2 || Issue-2 || May-Aug || Year-2024 || pp. 19-39

Reviewing the comparative thermal performance of solar air heaters with artificially roughened absorber plates

***¹Rohit Kumar Choudhary, ²Shubham Thakre, ³Anil Kumar, ⁴Anamika Thakur**

^{*1}Associate Professor, Bhopal Institute of Technology and Science, Bhojpur Road Bhopal, 462045 M.P. India
^{2, 3, 4} Student, Bhopal Institute of Technology and Science, Bhojpur Road Bhopal, 462045 M.P. India

**Corresponding Author: Rohit Kumar Choudhary
Email: bitshodme1@gmail.com*

Abstract:

Artificial roughness is often employed to augment heat transfer rates in solar air heaters. Extensive literature exists detailing diverse configurations and geometries of roughness elements, each yielding varying degrees of heat transfer effectiveness in terms of quality and quantity. This paper conducts a comprehensive review, examining both quantitative and qualitative aspects of heat transfer rates in artificially roughened solar air heaters across a spectrum of configurations. Analytical and experimental findings, alongside derived values utilizing equations or correlations established by researchers, are synthesized to evaluate heat transfer performance concerning roughness and flow parameters (p/e , e/D , and Re). Results indicate that multi V-roughness exhibits the highest average Nusselt number in experimental data, while end-of-side roughened solar air heaters yield maximum analytical Nusselt number values.

Keywords:

Relative roughness pitch (P/E), Relative roughness height (e/D), Flow Reynolds number (Re) and Average Nusselt number (Nu_r).

Nomenclature:

- A_c collector area, m²
- B** solar air heater duct height, m
- D** hydraulic diameter of solar air heater duct, m
- e** artificial roughness height, m
- g** heat transfer function
- R** roughness function
- e^+ roughness Reynolds number = $e / D \sqrt{\left(\frac{f_r}{2}\right)}$ (Prasad et. al. 2014)
- e^+ roughness Reynolds number = $e / D \sqrt{\left(\frac{\bar{f}}{2}\right)}$ (Prasad and Saini, 1991)
- e^{+opt} optimal roughness Reynolds number
 $= e/D \sqrt{\frac{f_r}{2}} Re = 23$ (Prasad et. al., 2015)
- e/D relative roughness height
- d/W relative gap position
- F' plate efficiency factor
- F_R heat removal factor
- f_s friction factor in four sided smooth duct
- f_r friction factor in four sided rough duct
- \bar{f} average friction factor = $(f_s + f_r) / 2$, in roughened collector.
- \bar{f}_r average friction factor in three sided rough duct(Prasad et. al., 2014)
- e/H baffle blockage ratio
- P/H baffle pitch spacing ratio
- B/s boosted Stanton number ratio
- g/e relative gap width
- H** solar air heater duct height, m (Referred cases)

h	convective heat transfer coefficient, $W/m^2 K$
L	collector length, m
l/e	relative long way length of mesh
\overline{Nu}	average Nusselt number for top side roughened duct
\overline{Nu}_r	average Nusselt number for three sided roughened duct (Prasad et.al., 2014)
Nu_r	Nusselt number for four sided smooth duct
p	roughness pitch, m
p/e	relative roughness pitch
P_r	Prandlt number
Re	Reynolds number
\overline{St}_r	average Stanton number for three sided roughened duct (Prasad et. al., 2014)
St	Stanton number for top side roughened duct
St_r	Stanton number in a four sided rough duct
s/e	relative short way length of mesh
W	solar air heater duct width, m
w	width of single V-rib
W/w	relative roughness width
W/H	aspect ratio of duct
U_L	overall heat transfer coefficient, $W/m^2 K$
ρ	fluid density, Kg/m^3
α	angle of attack ($^\circ$)
φ	chamfer/ wedge angle ($^\circ$)
$\varphi/90$	relative arc angle
η_{th}	thermal efficiency

1. Introduction:

Literature extensively covers the utilization of artificial roughness with varied geometries to amplify heat transfer in solar air heaters. For instance, Prasad and Mullick (1983) employed small diameter wires on the top absorber plate to enhance heat transfer in a solar air heater utilized for drying purposes. Additionally, Prasad and Saini (1988) analyzed the impact of protrusions, such as small diameter wires, on the absorber surface regarding heat transfer and friction factor for fully developed turbulent flow within a solar air heater duct. Further investigations conducted by Prasad (2013) explored the effects of relative roughness pitch values of 10, 15, and 20, alongside relative roughness heights of 0.020, 0.027, and 0.033, on heat transfer and friction. Notably, it was reported that the maximum Nusselt number and friction factor reached 2.38 and 4.25, respectively, for a relative roughness pitch of 10.

Prasad and Saini (1991) conducted an analysis aimed at optimizing the thermo-hydraulic performance of top-side artificially roughened solar air heaters, spanning a broad spectrum of relative roughness pitch (p/e), relative roughness height (e/D), and flow Reynolds number (Re). Their investigation concluded that the parameter roughness Reynolds number, denoted as e^+ , reaching a value of 24, yields optimal thermo-hydraulic performance.

Gupta et al. (1993) explored the effects of transverse wire-type roughness geometry affixed underneath an absorber plate. Their experiment encompassed aspect ratios ranging from 6.8 to 11.5, relative roughness heights ranging from 0.018 to 0.052, at a relative roughness pitch of 10, with roughness Reynolds numbers spanning 5 to 70 and Reynolds numbers ranging from 3000 to 18000. Results indicated an initial increase in Stanton number with rising Reynolds number up to 12000, followed by a decline with further increments.

In a subsequent study, Gupta et al. (1997) investigated the impact of transverse and inclined wire roughness on fluid flow characteristics in solar air heaters. They achieved maximum heat transfer coefficient at an angle of 60 degrees and a relative roughness pitch of 10. Their findings revealed that maximum enhancement in heat transfer coefficient occurred in roughened ducts at angles of 60 and 70 degrees, respectively. Furthermore, they identified roughened surfaces with a relative roughness height (e/D) of 0.033, corresponding to Reynolds numbers (Re) around 14000, as offering the best thermo-hydraulic performance within the investigated parameter range.

Saini and Saini (1997) conducted a study focusing on the heat transfer and friction characteristics within a solar air heater duct featuring a large aspect ratio, incorporating roughness in the form of expanded metal mesh geometry. Their investigation revealed that the average Nusselt number reached its maximum value at a relative longway mesh (L/e) of 46.87 and a relative shortway length (S/e) of 25, occurring at an angle of 61.90 degrees.

A comparative analysis of thermal performance was carried out by Muluwork et al. (1998) and Muluwork (2000) for roughened absorber plates fixed with staged discrete V-apex. They observed a boosted Stanton number ratio ranging between 1.32 and 2.47. Moreover, an increase in the relative roughness length ratio within the range of 3 to 7 led to a corresponding increment in the Stanton number.

(Karwa et al., 1999) formulated correlations for heat transfer coefficients and friction factors in solar air heater ducts featuring ribbed roughness.

(Verma and Prasad, 2000) experimentally verified for the optimal thermohydraulic performance in artificially roughened solar air heaters and arrived at the conclusion that the value of flow Reynolds number, $e^+ 24$, gives the optimal thermo hydraulic performance.

Bhagoria et al. (2002) applied wedge-shaped transverse repeated rib roughness to one broad heated wall of a solar air heater duct and collected data regarding friction and heat transfer. Their analysis revealed that the presence of wedge-shaped ribs resulted in a significant enhancement in the Nusselt number, approximately 2.4 times higher than that of a smooth duct. The Nusselt number exhibited an increasing trend, reaching its maximum value at a wedge angle of approximately 100 degrees, beyond which it sharply decreased with further increases in the wedge angle.

Saini and Saini (2008) investigated the performance of a solar air heater duct roughened with arc-shaped roughness elements. Through experimentation, they assessed the impact of various roughness parameters such as relative roughness height and relative arc angle on the heat transfer coefficient across a range of Reynolds numbers (Re) from 2000 to 17000, relative roughness heights (e/D) from 0.0213 to 0.0422, and relative arc angles ($\alpha/90$) from 0.3333 to 0.6666. Their findings indicated a maximum enhancement in the Nusselt number of up to 3.80 times that of a smooth surface, corresponding to a relative arc angle of 0.3333 and a relative roughness height of 0.0422.

Varun et al. (2008) conducted experimental investigations utilizing a combination of transverse and inclined ribs as roughness geometry to examine the thermal performance across

a range of Reynolds numbers (Re) from 2000 to 14000, rib pitches (p) from 5 to 13 mm, roughness heights (e) of 1.6 mm, and aspect ratios (W/H) of 10. Their results demonstrated that collectors roughened with this type of roughness exhibited optimal performance at a relative roughness pitch (p/e) of 8.

Table I provides a summary of various roughness geometries, including transverse or inclined ribs, wedge-shaped ribs, rib-grooved, dimple-shaped, arc-shaped wire, compound turbulation, metal grit ribs, and W-shape deals, for the analysis and investigation toward enhancing heat transfer in solar air heaters.

Momin et al. (2002) conducted experiments on flow through a duct roughened with V-shaped ribs attached to the underside of one broad wall of the duct, aimed at gathering data on heat transfer and fluid flow characteristics. Their observations indicated that the Nusselt number increased with rising Reynolds numbers. Specifically, for a relative roughness height of 0.034 and an angle of attack of 60 degrees, the V-shaped ribs enhanced Nusselt number values by 1.14 and 2.3 times, respectively, compared to inclined ribs and a smooth plate case at a Reynolds number of 17034.

Sahu and Bhagoria (2005) investigated the effect of 90-degree broken transverse ribs on heat and fluid flow characteristics, employing a roughness height of 1.5 mm, an aspect ratio of 8, pitches ranging from 10 to 30 mm, and Reynolds numbers ranging from 3000 to 12000. The rate of heat transfer was enhanced by 1.25 to 1.4 times over a smooth duct, with a maximum thermal efficiency of 83.5% observed during experimentation.

Varun et al. (2007) provided a review of roughness geometries used in solar air heaters. Aharwal et al. (2008) investigated the thermo-hydraulic performance of a solar air heater featuring inclined continuous ribs with a gap, considering parameters such as $W/H=5.84$, $p/e=10$, $e/D_h=0.0377$, $\alpha=60$ degrees, $g/e=0.5-2$, $d/W=0.1667-0.667$, and Reynolds numbers ranging from 3000 to 118000. They found that at optimum parameter values ($g/e=0.5$ and $d/W=0.25$), the increase in Nusselt number and friction factor reached maximum values of 2.59 and 2.87, respectively.

Bopche and Tandale (2009) investigated the thermo-hydraulic performance of solar air heaters featuring inverted U-shaped ribs on the absorber plate. They found these roughness elements to be efficient even at lower Reynolds numbers ($Re < 5000$), with turbulence created primarily in the viscous sub-layer, resulting in higher thermo-hydraulic performance compared to smooth solar air heaters.

Hans et al. (2009) reviewed the performance of artificially roughened solar air heaters, while Hans et al. (2010) developed multiple V-rib roughness and conducted extensive experimentation to gather data on heat transfer and fluid flow characteristics of a roughened duct. They observed maximum enhancements in Nusselt number and friction factor due to the presence of multi V-rib roughness, reaching 6 and 5 times, respectively, compared to a smooth duct. Maximum enhancement in heat transfer was achieved corresponding to a relative roughness width (W/w) of 6, with Nusselt number reaching its maximum value at a 60-degree angle of attack.

Sharma et al. (2010) concluded that small diameter protrusion wires exhibit superior performance within flow Reynolds numbers limited to 10000. Sethi et al. (2010) predicted the effective efficiency of solar air heaters using discrete ribs.

Promvongse (2010) conducted an experimental investigation to assess turbulent forced convection heat transfer and friction losses behavior in air flow through a channel fitted with multiple 60-degree V-baffle tabulators. The experiment utilized a channel with an aspect ratio of 10 and a height of 30 mm, featuring three different baffle blockage ratios (0.10, 0.20, and 0.30) and three baffle pitch spacing ratios (1, 2, and 3), while keeping the transverse pitch of the V-baffle constant.

Kumar et al. (2011) investigated the enhancement of heat transfer coefficient in a solar air heater equipped with a roughened air duct featuring inclined discrete ribs at 60 degrees. They identified that maximum heat transfer enhancement occurred for a relative roughness pitch of 12, relative gap position of 0.35, and relative roughness height of 0.0498. Statistical correlations for friction factor and Nusselt number were derived as functions of gap position, rib depth, pitch, and Reynolds number, with average absolute standard deviations of 3.4% and 3.8%, respectively.

Lanjewar et al. (2011) conducted an experimental investigation on heat transfer and friction factor in a rectangular duct featuring W-shaped ribs arranged at an inclination to the flow direction. The duct had a width-to-height ratio of 8, a relative roughness pitch of 10, a relative roughness height of 0.03375, and a flow angle of attack ranging from 30 to 75 degrees.

Patil et al. (2012) reviewed various types of roughness geometries and investigation techniques employed in artificially roughened solar air heaters. They noted that provision of artificial roughness, such as thin wires of varying diameters at different relative roughness pitches and heights on the absorber plate, led to increased heat transfer coefficients and thermal efficiency compared to smooth surfaces.

Chamoli et al. (2012) conducted a comprehensive review focusing on future research directions concerning the utilization of turbulence promoters for enhancing heat transfer in solar air heaters, along with assessing the performance of double pass solar air heaters.

Bhusan et al. (2012) developed the thermal and thermo-hydraulic performance of protruded solar air heaters.

Karwa et al. (2013) established correlations for Nusselt number and friction factor for multi V-shaped roughness in solar air heaters, observing a 12.5-20% enhancement in thermal efficiency with 60-degree V-down discrete rib roughnesses.

Saurabh et al. (2013) conducted a review on heat transfer and thermal efficiency in solar air heaters featuring artificial roughness.

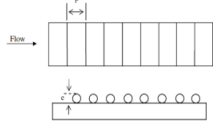
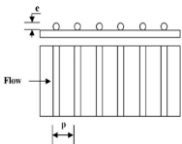
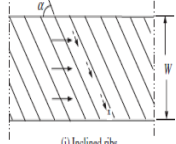
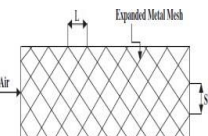
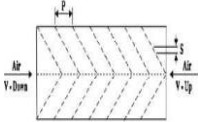
Prasad (2013) presented experimental results on heat transfer and thermal performance of artificially roughened solar air heaters under fully developed turbulent flow conditions. These solar air heaters demonstrated significantly higher values of collector heat removal factor (F_{RC}), collector efficiency factor (F_{RC}), and thermal efficiency (η_{th}) compared to smooth collectors. Across the investigated operating parameters, the ratios of these parameters for roughened collectors to smooth collectors were found to be 1.786, 1.806, and 1.842, respectively.

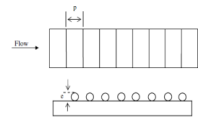
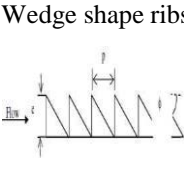
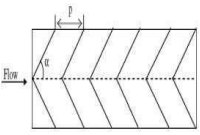
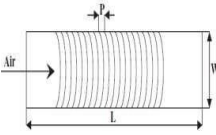
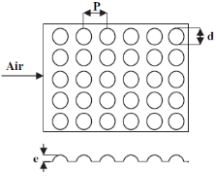
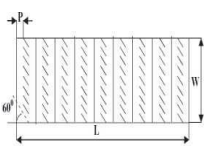
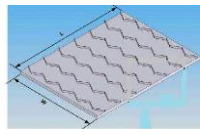
Prasad et al. (2014) conducted an analysis concerning fluid flow and heat transfer in a novel solar air heater configuration featuring artificial roughness applied to three sides (the two side walls and the top side) of the rectangular duct, which also included glass covers on three sides. They developed equations for friction factor and heat transfer parameters. Analytical values of the friction factor and heat transfer parameter were found to be 2 to 40% higher and 20 to 75% higher, respectively, compared to the values reported by Prasad and Saini (1988) for the same range of operating parameters (p/e , e/D , and Re) and fixed values of W and B .

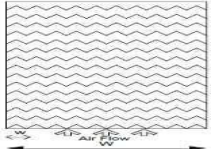
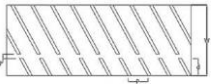
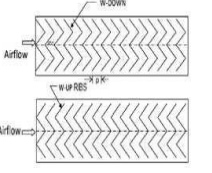
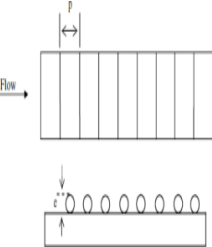
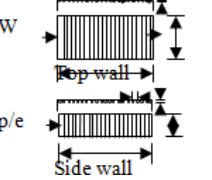
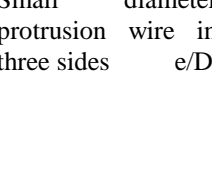
Prasad et al. (2015) analyzed the thermo-hydraulic optimization of the same three-sided artificially roughened solar air heater to maximize heat transfer while minimizing pumping power (friction factor). They determined that the optimal thermo-hydraulic performance condition corresponds to the optimal value of roughness Reynolds number (Re_+), for a specific set of roughness and flow parameters (p/e , e/D , and Re).

Table. 1 presents various roughness geometries, fluid flow directions, and the analyzed roughness and flow parameters, along with the equations developed for heat transfer and friction parameters by different authors, providing a comparative view of the research landscape.

Table. 1

S. No	Reference	Roughness Geometry	Parameter Investigated	Associated Equations / Correlations
1	Prasad and Saini (1988)	Small diameter protrusion wire 	$e/D=0.020-0.033$ $p/e=10-20$ $Re=5000-50000$	$\bar{S}_t = \frac{\bar{f}/2}{1 + \sqrt{\frac{\bar{f}}{2} [4.5(\epsilon^+)^{0.222} Pr^{0.57} - 0.95(\rho/\epsilon)^{0.222}]}}$ $\bar{f} = \frac{(W + 2B)f_s + W \left[\frac{2}{\{0.95(\rho/\epsilon)^{0.222} + 2.5 \ln(D/2\epsilon) - 3.75\}^2} \right]}{2(W + B)}$ $\overline{Nu} = \bar{S}_t Re Pr$
2	Gupta et al., (1993)	Transverse ribs 	$e/D=0.018-0.052$ $Re=3000-18000$ $W/H=6.8-11.5$	$Nu = 0.000824(\epsilon/D)^{-0.712}(W/H)^{0.224} Re^{1.062}$ For For
3	Gupta et al., (1997)	Inclined ribs  (i) Inclined ribs	$e/D=0.020-0.053$ $p/e=7.5 \text{ \& } 10$ $=30-90$ $Re=5000-30000$	For For $\bar{f} = 0.06412(\epsilon/D)^{0.019}(W/H)^{0.227}(Re)^{-0.125}$
4	Saini and Saini (1997)	Wire mesh roughness 	$e/D=0.012-0.039$ $S/e=15.62-46.87$ $L/e=25.00-71.87$ $Re=1900-13000$	$\overline{Nu} = 4.0 \times 10^{-4} Re^{1.222} (\epsilon/D)^{0.222} (S/10e)^{0.222} \times \exp[-1.222 \ln(S/10e)] (L/10e)^{1.222} \times \exp[-1.222 \ln(L/10e)]$ $\bar{f} = 0.815(Re)^{0.222} (S/10e)^{0.222} (10e/d)^{0.591}$
5	Mulluwork et al., (1998)	V shaped staggered discrete wire ribs 	$e/D=0.02B/s=3-9$ $=60^0$ $Re=2000-15500$	$Nu = 0.00534(B/s)^{1.2498} Re^{1.2991}$ $f = 0.7117(B/s)^{0.0626} Re^{-1.991}$
		Transverse Protrusion wire		$Nu = 0.08596(\rho/\epsilon)^{-0.054} (\epsilon/D)^{0.072} Re^0$

6	Verma and Prasad(2000)		$e/D=0.01-0.03$ $p/e=10-40$ $Re=5000-20000$ $e^+=8-42$ $P_r=0.7$	For, For,
7	Bhagoria et al., (2002)	Wedge shape ribs 	$e/D=0.015-0.033=8,10,12,15$ $Re=3000-8000$	$\overline{Nu} = 1.89 \times 10^{-4} Re^{0.71} (\epsilon/D)^{0.415} (P/\epsilon)^{0.214} \times \exp[-0.71 \ln(P/\epsilon)] (\phi/10)^{-0.022} \times \exp[-1.4 \ln(\phi/10)]$ $\bar{f} = 12.44 (\epsilon/D)^{0.222} (\phi/10)^{0.422} Re^{-0.122} (P/\epsilon)^{-0.22}$
8	Momin et al., (2002)	V-shape ribs 	$e/D=0.02-0.034$ $p/e=10$	$\overline{Nu} = 0.067 Re^{0.3333} (\epsilon/D)^{0.424} (\alpha/60)^{-0.077} \times \exp[-0.719 \ln(\alpha/60)^2]$ $\bar{f} = 6.266 (\epsilon/D)^{0.255} (\alpha/60)^{-0.072} Re^{-0.422} \exp[-0.719 \ln(\alpha/60)^2]$
9	Saini and Saini (2008)	Arc shape roughness 	$e/D=0.0213-0.0422$ $p/e=10$ $Re=2000-17000$ $\alpha/90=0.333-0.666$ $W/H=12$	$\overline{Nu} = 0.001047 Re^{1.2122} (\epsilon/D)^{0.2772} (\alpha/90)^{-0.1132}$ $\bar{f} = 0.14408 (\epsilon/D)^{0.1765} (\alpha/90)^{0.1225} Re^{-0.17102}$
10	Saini et al., (2008)	Dimple shape roughness 	$e/D=0.0189-0.038$ $p/e=8-12$ $Re=2000-12000$	$\overline{Nu} = 5.2 \times 10^{-4} Re^{0.71} (P/\epsilon)^{0.115} \times [\exp(-2.21) \{\ln(P/\epsilon)\}^2] (\epsilon/D)^{0.212} \times [\exp(-1.30) \{\ln(\epsilon/D)\}^2]$ $\bar{f} = 0.0642 (Re)^{-0.422} (\epsilon/D)^{-0.0214} (P/\epsilon)^{-0.485} \exp[0.054 \{\ln(P/\epsilon)\}^2]$ $\exp[-0.840 \{\ln(\epsilon/D)\}^2]$
11	Varun et al., (2008)	Combined inclined and transverse ribs 	$e/D=0.030$ $p/e=8$ $W/H=10$ $Re=2000-14000$	$\bar{f} = 1.0858 (Re)^{-0.2885} (P/\epsilon)^{0.0214}$ $\overline{Nu} = 0.0006 (Re)^{1.212} (P/\epsilon)^{0.02104}$
12	Promvonge, (2010)	Multiple V shaped baffles 	$e/H=0.1, 0.2$ and 0.3 $P/H=1, 2$ and 3 $Re=5000-25000$	$Nu = 0.147 Re^{0.722} (P/H)^{0.4} (1 - \epsilon/H)^{-1.722} (1 + P/H)^{-0.42}$ $f = 0.48 Re^{0.022} (1 - \epsilon/H)^{-1.422} (1 + P/H)^{-0.022}$

13	Hans et al., (2010)	<p>Multi V-rib roughness</p> 	<p>e/D=0.019-0.043 p/e=6-12 Re=2000-20000 α=30-75 W/w=1-10</p>	$\overline{Nu} = 3.85 \times 10^{-4} Re^{0.41} (e/D)^{0.27} (W/w)^{0.44} (p/e)^{-0.49} \times \exp[-0.117 \ln(P/e)] \times \exp[-0.11 \ln(W/w)] \times \exp[-0.11 \ln(p/e)]$ $\bar{f} = 4.47 \times 10^{-4} Re^{-0.1133} (e/D)^{0.27} (W/w)^{0.22} (p/e)^{-0.22} \times \exp[-0.52 \ln(\frac{D}{2e})] (P/e)^{0.22} \exp[-2.133 \ln(P/e)]$
14	Kumar et al., (2011)	<p>600 angle inclined continuous discrete rib</p> 	<p>Re=4105.2-20526.2 e/D=0.0249, 0.0374 and 0.0498 p/e=8, 12 and 16 d/W=0.15, 0.25 and 0.35 g/e=1</p>	$Nu = 3 \times 10^{-2} Re^{0.54} (e/D)^{0.22} (P/e)^{0.58} (d/W)^{0.115} \times \exp[-1.237 \ln(P/e)^2]$ $f = 0.0014 Re^{-0.22} (e/D)^{0.22} (P/e)^{0.58} (d/W)^{0.097} \times \exp[-0.944 \ln(P/e)^2]$
15	Lanjewar et al., (2011)	<p>W-shaped ribs</p> 	<p>p/e=10 e=1.5 e/D=0.03375 W/H=8 Re=2300-14000 =300,450,600-750 e+=8-44</p>	$R = \sqrt{(2/f)} + 2.5 \ln(2e/D) + 3.75$ $e^+ = \sqrt{(f/2)} Re (e/D)$ $g = [(f/2St) - 1] \sqrt{(2/f)} + R$
16	Prasad (2013)	<p>Transverse rib roughness</p> 	<p>e/D=0.0092-0.0279 p/e=10-40 Re=2959-12631</p>	$\overline{Nu} = (\bar{f}/2) Re Pr / \left[1 + \sqrt{(\bar{f}/2)} \{ 4.5(e^+)^{0.22} Pr^{0.57} - 0.95(P/e)^{0.52} \} \right]$ $\bar{f} = \frac{2}{[0.95(P/e)^{0.52} + 2.5 \ln(D/2e) - 3.75]^2}$
17	Prasad et al., (2014)	<p>Small diameter protrusion wire in three sides e/D</p> 	<p>e/D=0.020-0.033 p/e=10-20 Re=3000-12000</p>	$\overline{Nu}_s = \frac{\bar{f}/2}{1 + \sqrt{(\bar{f}/2)} [4.5(e^+)^{0.22} Pr^{0.57} - 0.95(P/e)^{0.52}]}$ $\bar{f}_s = \frac{(W + 2B) \left[\frac{2}{[0.95(P/e)^{0.52} + 2.5 \ln(D/2e) - 3.75]^2} \right] + Wf_s}{2(W + B)}$
18	Prasad et al., (2015)	<p>Small diameter protrusion wire in three sides e/D</p> 	<p>e/D=0.01126-0.0279 p/e=10-40 Re=3000-20000</p>	$\bar{St}_s = \frac{\bar{f}_s/2}{1 + \sqrt{(\bar{f}_s/2)} [4.5(e^+)^{0.22} Pr^{0.57} - 0.95(P/e)^{0.52}]}$ $e^+ = \frac{e/D \sqrt{\bar{f}_s}}{2} Re$ <p>For optimal condition,</p>

			$e_{opt}^+ = \frac{e/D \sqrt{f_r}}{2} Re = 23$
--	--	--	--

Table 2: Comparison of enhancement in heat transfer data (\overline{Nu} & \overline{f} , f_r)

References	Reynolds Number	Average Nusselt Number		Average Friction Factor	
		Values	Remarks	Values	Remarks
Prasad et al (2014)	(3-14)X10 ³	40-140	Analytical	0.047-0.035	Analytical
Bhagoria (2002)	(3-14)X10 ³	18-82	Analytical	0.03-0.0264	Analytical
Prasad & Saini (1998)	(3-14)X10 ³	20-65	Analytical	0.03-0.025	Analytical
Gupta et al (1993)	(3-14)X10 ³	10-30	Analytical	0.037-0.019	Analytical
Saini & Saini (1997)	(3-14)X10 ³	20-120	Analytical	0.039-0.027	Analytical
Hans et al (2010)	(3-14)X10 ³	50-185	Experimental	0.049-0.027	Experimental
Momin et al (2002)	(3-14)X10 ³	20-70	Experimental	0.013-0.007	Experimental
Prasad (2013)	(3-14)X10 ³	20-65	Experimental	-----	-----
Saini & Saini (2008)	(3-14)X10 ³	10-65	Experimental	0.018-0.014	Experimental
Saini et al (2008)	(3-14)X10 ³	8-50	Experimental	0.07-0.045	Experimental
Varun et al (2008)	(3-14)X10 ³	9-32	Experimental	0.03-0.019	Experimental

Table 3: Value of e_{opt}^+ different roughness geometries for fully developed turbulent flow

S.No.	References	Roughness Geometry Type	p/e	e/D	Re	e_{opt}^+
1.	Sheriff and Gumley (1966)	Annulus with wires	10	—	10 ⁴ -2×10 ³	35

2.	Webb and Eckert (1972)	Rectangular	10-40	0.01-0.04	$6-100 \times 10^3$	20
3.	Lewis (1975a, 1975b)	Circular tubes with ribs	2-60	0.02-0.1	—	20
4.	Prasad and saini (1991)	Rectangular duct with thin wires on one side	10-40	0.020-0.033	$3-20 \times 10^3$	24
5.	Prasad et al., (2015)	Rectangular duct with thin wires on three sides	10-40	0.01126-0.0279	$3-20 \times 10^3$	23

Table. 3 displays various values of the optimal roughness Reynolds number, $e+_{opt}$ as documented in literature, encompassing diverse roughness geometries and a spectrum of roughness and flow parameter values pertinent to fully developed turbulent flow.

2. Results and discussion:

Research on artificially roughened solar air heater ducts has primarily focused on examining the impact of roughness element shape and arrangement on heat transfer requirements through comparative assessments. Hence, it is logical to individually evaluate the performance of various roughness geometries concerning heat transfer.

Fig. 1 and Fig. 2 have been constructed using the derived heat transfer data, \overline{Nu} and \overline{f} , \overline{fr} respectively. These values were obtained by substituting the roughness and flow parameters into equations established by the respective authors. The plots illustrate the variation in average Nusselt number and average friction factor as functions of Reynolds number for different roughness geometries, as analytically developed by various researchers. A significant increase in both Nusselt number and friction factor is observed across all cases.

Fig. 1 highlights that the Nusselt number attains its maximum value when employing

Transverse ribs on all three sides (the two sidewalls and the top surface) of the artificially roughened solar air heater duct, whereas it reaches its minimum with inclined ribs across all Reynolds number values. Notably, transverse rib roughness on all three sides demonstrates superior performance among the various roughness geometries, yielding nearly double the enhancement in heat transfer rates compared to alternative configurations.

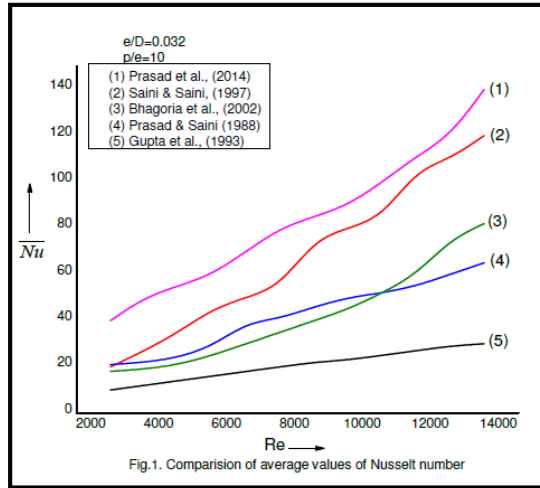


Figure. 1

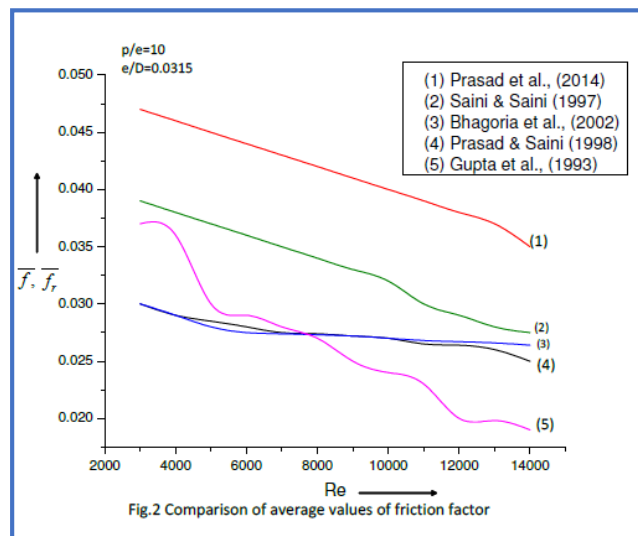


Figure. 2

Fig. 3 and 4 depict the experimental results for heat transfer data corresponding to various roughness geometries tested by different researchers. The graphs illustrate the relationship between average Nusselt number and average friction factor as a function of Reynolds number. It is evident that among the tested roughness geometries, the multi V shape exhibits the highest Nusselt number, while the combination of transverse and inclined ribs shows the lowest Nusselt number across all Reynolds numbers.

Specifically, the multi V shape roughness consistently demonstrates superior heat transfer performance compared to other geometries. Analysis reveals a notable increase in Nusselt number for V shape rib, multi V shape rib, inclined rib, and transverse rib roughness, followed by a slight reduction in the rate of increase.

Considering applications with higher flow rates, employing wire mesh or arc shape roughness is preferable for maximizing heat transfer rates. Conversely, for systems operating at low to moderate flow rates, multi V shape roughness proves to be the optimal choice for enhancing heat transfer efficiency.

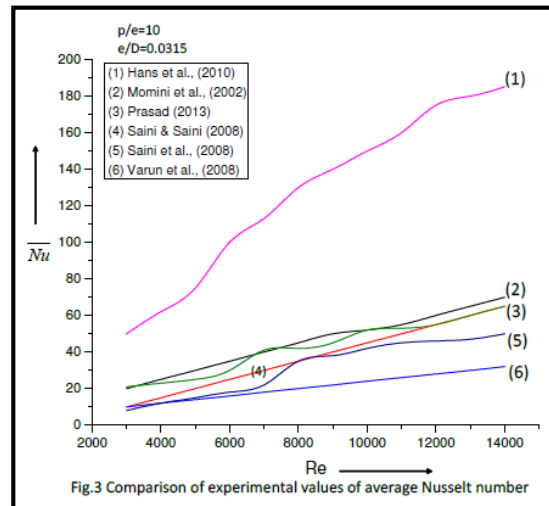


Figure. 3

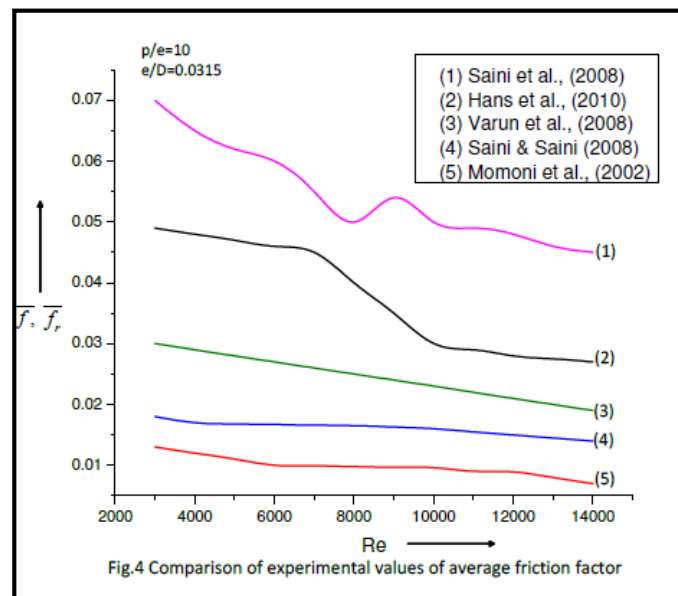


Figure. 4

Furthermore, incorporating gaps in geometries such as V shape rib and multi V shape rib can significantly enhance heat transfer rates compared to continuous V or multi V ribs. This enhancement is attributed to the presence of secondary flow cells, with multi V rib roughness generating multiple secondary flow cells, resulting in the highest heat transfer augmentation.

In summary, the choice of roughness geometry plays a crucial role in heat transfer enhancement, with multi V shape rib roughness offering substantial benefits due to its ability to generate multiple secondary flow cells and maximize heat transfer rates, particularly in Systems operating at low to moderate flow rates.

3. Conclusion:

- Employing artificial roughened surfaces with various roughness geometries emerges as the most effective method for augmenting heat transfer rates from heated surfaces to flowing fluids, albeit with a moderate increase in fluid friction.
- Among the tested roughness geometries, multi V rib roughness exhibits notable performance in solar air heaters, offering distinct advantages in enhancing heat transfer rates.
- Analytically developed roughness geometries, particularly the application of artificial roughness on three sides of the absorber plate (top side and two side walls), demonstrate superior heat transfer rates in solar air heaters.
- Experimentations involving rib roughened ducts utilizing roughened plates, whether through fixation of wires or machining on metallic plates, appear outdated. These techniques entail laborious fabrication processes, elevated costs, and prolonged durations, rendering them less favorable in contemporary applications.

4. References:

- (1) K. R. Aharwal, B. K. Gandhi, and J. S. Saini, "Experimental investigation on heat transfer enhancement due to a gap in an inclined continuous rib arrangement in a rectangular duct of solar air heater," *Renewable Energy*, vol. 33, pp. 585-596, 2008.
- (2) J. S. Bhagoria, J. S. Saini, and S. C. Solanki, "Heat transfer coefficient and friction factor correlation for rectangular solar air heater duct having transverse wedge shaped rib roughness on the absorber plate," *Renewable Energy*, vol. 25, pp. 341-369, 2002.
- (3) B. Bhushan and R. Singh, "Thermal and thermohydraulic performance of roughened solar air heater having protruded absorber plate," *International Journal of Solar Energy*, vol. 86, issue 11, pp. 3388-3396, 2012.

- (4) Santosh B. Bopche and Madhukar S. Tandale, "Experimental investigation on heat transfer and frictional characteristics of a tabulator roughened solar air heater duct," *International Journal of Heat Mass Transfer*, vol. 52, pp. 2834-2848, 2009.
- (5) S. Chamoli, R. Chauhan, N. S. Thakur, and J. S. Saini, "A review of the performance of double pass solar air heater," *International Journal of Renewable and Sustainable Energy Reviews*, vol. 16, issue 10, pp. 481- 492, 2012.
- (6) S. Chamoli, N. S. Thakur, and J. S. Saini, "A review of turbulence promoters used in solar thermal system," *International Journal of Renewable and Sustainable Energy Reviews*, vol. 16, issue 5, pp. 3154- 3175, 2012.
- (7) D. Gupta, S. C. Solanki, and J. S. Saini, "Heat and fluid flow in rectangular solar air heater ducts having transverse rib roughness on absorber plate," *Sol. Energy*, vol. 51, pp. 31-37, 1993.
- (8) D. Gupta, S. C. Solanki, and J. S. Saini, "Thermo hydraulic performance of solar air heaters with roughened absorber plates," *Solar Energy*, vol. 61, issue 1, pp. 33-42, 1997.
- (9) V. S. Hans, R. P. Saini, and J. S. Saini, "Performance of artificially roughened solar air heater-A review," *Renewable and Sustainable Energy Reviews*, vol. 13, pp. 1854-1869, 2009.
- (10) V. S. Hans, R. P. Saini, and J. S. Saini, "Heat transfer and friction factor correlations for a solar air heater duct roughened artificially with multiple V-ribs," *Solar Energy*, vol. 84, pp. 898-911, 2010.
- (11) A. R. Jaurker, J. S. Saini, and B. K. Gandhi, "Heat transfer and friction characteristics of rectangular solar air heater duct using rib-grooved artificial roughness," *Solar Energy*, vol. 80, pp. 895-907, 2006.
- (12) A. Karwa, R. P. Saini, and J. S. Saini, "Development of correlation for Nusselt number and friction factor for solar air heater with roughened duct having multi v-shaped with gap rib and artificial roughness," *International Journal of Renewable Energy Research*, vol. 58, pp. 151- 163, 2013.
- (13) R. Karwa, S. C. Solanki, and J. S. Saini, "Heat transfer coefficient and friction factor correlation for the transitional flow regimes in rib-roughened rectangular duct," *International Journal of Heat Mass Transfer*, vol. 42, pp. 1597-1615, 1999.
- (14) R. Karwa, "Experimental studies of augmented heat transfer and friction in

- asymmetrically heated rectangular ducts with ribs on the heated wall in transverse, inclined, V-continuous and V-discrete pattern,” *International Communications in Heat and Mass Transfer*, vol. 30, issue 2, pp. 241-250, 2003.
- (15) R. Karwa, and G. Chitoshiya, “Performance study of solar air heater having V-down discrete ribs on absorber plate,” *International Journal of Energy*, vol. 55, pp. 939-955, 2013.
 - (16) S. T. Kumar, V. Mittal, N. S. Thakur, and A. Kumar, “Heat transfer and friction factor correlations for rectangular solar air heater duct having 600 inclined continuous discrete rib arrangement,” *British Journal of Applied Science & Technology*, vol. 3, pp. 67-93, 2011.
 - (17) A. Layek, J. S. Saini, and S. C. Solanki, “Effect of chamfering on heat transfer and friction characteristics of solar air heater having absorber plate roughened with compound turbulators,” *Renewable Energy*, vol. 34, pp. 1292-1298, 2009.
 - (18) A. Lanjewar, J. L. Bhagoria, and R. M. Sarviya, “Experimental study of augmented heat transfer and friction in solar air heater with different orientations of W-rib roughness,” *Experimental Thermal and Fluid Science*, vol. 35, pp. 986-995, 2011.
 - (19) M. J. Lewis, “An elementary analysis for predicting the momentum and heat transfer characteristics of hydraulically rough surface,” *Trans. ASME Journal of Heat Transfer*, vol. 97, pp. 249-254, 1975.
 - (20) M. J. Lewis, “Optimizing the thermo hydraulic performance of rough surfaces,” *International Journal of Heat Mass Transfer*, vol. 18, pp. 1243-1248, 1975.
 - (21) AME Momin, J. S. Saini, and S. C. Solanki, “Heat transfer and friction in solar air heater duct with V-shaped rib roughness on absorber plate,” *International Journal Heat Mass Transfer*, vol. 45, pp. 3383–3396, 2002.
 - (22) K. B. Mulluwork, J. S. Saini, and S. C. Solanki, “Studies on discrete rib roughness solar air heaters,” in *Proceeding of National Solar Energy convention*, pp. 75-84, 1998.
 - (23) K. B. Mulluwork, “Investigations on fluid flow and heat transfer in roughened absorber solar heaters,” *PhD thesis, IIT Roorkee*, 2000.
 - (24) A. K. Patil, J. S. Saini, and K. Kumar, “A comprehensive review on roughness geometries and investigation techniques used in artificially solar air heaters,” *International Journal of Renewable Energy Research*, vol. 2, pp. 1-15, 2012.

- (25) K. Prasad and S. C. Mullick, "Heat transfer characteristics of a solar air heater used for dry purposes," *Applied Energy*, vol. 13, pp. 83-85, 1983.
- (26) B. N. Prasad and J. S. Saini, "Effect of artificial roughness on heat transfer and friction factor in a solar air heater," *Solar Energy*, vol. 41, pp. 555-560, 1988.
- (27) B. N. Prasad, J. S. Saini, "Optimal thermo-hydraulic performance of artificially roughened solar air heaters," *Solar Energy*, vol. 47, pp. 91- 96, 1991.
- (28) B. N. Prasad, "Thermal performance of artificially roughened solar air heaters," *Solar Energy*, vol. 91, pp. 59-67, 2013.
- (29) B. N. Prasad, Arun K. Behura, and L. Prasad, "Fluid flow and heat transfer analysis for heat transfer enhancement in three sided artificially roughened solar air heater," *Solar Energy*, vol. 105, pp. 27-35, 2014.
- (30) B. N. Prasad, Ashwini Kumar, and K. D. P. Singh, "Optimization of thermo hydraulic performance in three sides artificially roughened solar air heaters," *Solar Energy*, vol. 111, pp. 313-319, 2015.
- (31) P. Promvongse, "Heat transfer and pressure drop in a channel with multiple 600 V-baffles," *International Communications in Heat and Mass Transfer*, vol. 37, pp. 835-840, 2010.
- (32) M. M. Sahu, and J. L. Bhagoria, "Augmentation of heat transfer coefficient by using 900 broken transverse ribs on absorber plate of solar air heater," *Renewable Energy*, vol. 30, pp. 2063-2075, 2005.
- (33) R. P. Saini, and J. S. Saini, "Heat transfer and friction factor correlations for artificially roughened duct with expanded metal mesh as roughness element," *International Journal of Heat Mass Transfer*, vol. 40, pp. 973- 986, 1997.
- (34) S. K. Saini, and R. P. Saini, "Development of correlations for Nusselt number and friction factor for solar air heater with roughened duct having arc-shaped wire as artificial roughness," *Solar Energy*, vol. 82, pp. 1118-1130, 2008.
- (35) R. P. Saini, and J. Verma, "Heat transfer and friction correlations for a duct having dimple shape artificial roughness for solar air heater," *Energy*, vol. 33, issue 8, pp. 1277-1287, 2008.
- (36) S. Saurabh, and M. M. Sahu, "Heat transfer and thermal efficiency of solar air heater having artificial roughness: A review," *International Journal of Renewable Energy*

- Research*, vol. 3, issue 3, pp. 498-508, 2013.
- (37) N. Sheriff, and P. Gumley, "Heat transfer and friction properties of surfaces with discrete roughness," *International Journal of Heat Mass Transfer*, vol. 9, pp. 1297-1320, 1966.
- (38) M. Sethi, M. Sharma, and Varun, "Effective efficiency prediction for diameter type of ribs used in solar air heater," *International Journal of Energy and Environment*, vol. 1, issue 2, pp. 333-342, 2010.
- (39) M. Sharma and Varun, "Performance estimation of artificially roughened solar air heater duct provided with continuous ribs," *International Journal of Energy and Environment*, vol. 1, issue 5, pp. 897-910, 2010.
- (40) Varun, R. P. Saini, and S. K. Singal, "A review on roughness geometry used in solar air heaters," *Solar Energy*, vol. 81, pp. 1340-1350, 2007.
- (41) Varun, R. P. Saini, and S. K. Singal, "Investigation on thermal performance of solar air heaters having roughness elements as a combination of inclined and transverse ribs on the absorber plate," *Renewable Energy*, vol. 33, pp. 1398-1405, 2008
- (42) S. K. Verma and B. N Prasad, "Investigation for the optimal thermo hydraulic performance of artificially roughened solar air heaters," *Renewable Energy*, vol. 20, pp. 19-36, 2000.
- (43) R. L. Webb and E. R. G. Eckert, "Application of rough surfaces to heat exchanger design," *International Journal of Heat Mass Transfer*, vol. 15, pp. 1647-1658, 1972.